Gold/Platinum Bimetallic Core/Shell Nanoparticles Stabilized by a Fréchet-Type Dendrimer: Preparation and Catalytic Hydrogenations of Phenylaldehydes and Nitrobenzenes

Wei Zhang · Lei Li · Yukou Du · Xiaomei Wang · Ping Yang

Abstract Au/Pt bimetallic core/shell nanoparticles that were stabilized by polyaryl ether trisacetic acid ammonium chloride dendrons (G_3NACl) were synthesized and used as catalysts for the hydrogenation of 3-phenoxybenzaldehyde to 3-phenoxyphenyl methanol and nitrobenzenes to anilines. Transmission electron microscopy (TEM), X-ray diffraction (XRD), and UV-visible absorption spectroscopy revealed that Au/Pt bimetallic nanoparticles with a 6-nm Au core and average overall diameters of 9.0 ± 2.4 nm, 10.4 ± 2.8 nm, and 13.0 ± 3.2 nm for $Au_{75}Pt_{25}@G_3NACl$, $Au_{50}Pt_{50}@G_3NACl$, and $Au_{25}Pt_{75}@G_3NACl$, respectively, had formed. Au/Pt bimetallic nanoparticles showed higher catalytic activity for the hydrogenation of nitrotoluenes to anilines and 3-phenoxybenzaldehyde to 3-phenoxyphenyl methanol as compared to monometallic platinum nanoparticles and physical mixtures of monometallic Pt and Au nanoparticles. The higher activity of the Au/Pt bimetallic nanoparticles may be attributed to the fact that the gold core attracts electrons from platinum. The electron-deficient platinum shell may favor the adsorption of the substrate with polar carboxyl groups.

Keywords Au/Pt bimetallic core/shell nanoparticles · Fréchet-type dendrimers · 3-Phenoxy benzaldehyde · Nitrobenzenes · Catalytic hydrogenation

W. Zhang · L. Li · Y. Du · X. Wang · P. Yang (✉)
College of Chemistry and Chemical Engineering,
Suzhou University, Suzhou 215123, China
e-mail: pyang@suda.edu.cn

W. Zhang
School of Chemical and Materials Engineering,
Jiangnan University, Wuxi 214122, China

1 Introduction

Bimetallic nanoparticles are important in catalysis because of the synergic interaction between two different metallic elements contained in one particle, which leads to enhanced catalytic activity and selectivity that is distinct from those of the corresponding monometallic particles [1–12]. Organic polymers are usually used as stabilizers to prevent metal nanoparticles from agglomeration and precipitation during the stages of chemical preparation and catalysis. Rampind and Nord used polyvinyl alcohol (PVA) as a stabilizer to prepare Pd and Pt colloidal catalysts. These colloidal catalysts were efficient in a water gas shift reaction and the hydrogenations of organic compounds [13]. Since then, many different polymers, especially various dendrimers, were exploited and used as stabilizers or templates for nanoparticle preparations [14–36]. According to previous studies, Au/Ag (alloy or core/shell) and Pd/Pt bimetallic nanoparticles that are 1–3 nm in size can be synthesized using Polyamidoamine (PAMAM) dendrimers as stabilizers [37–39]. Monometallic Pt, bimetallic Pt/Pd, and Pt/Au nanoparticles that were stabilized by cubic silsesquioxanes were also prepared and used as hydrogenation catalysts. These metallic catalysts can be separated from the system after the cessation of the catalytic reactions and reused by simply adjusting the pH of the solution [34, 40]. Using Fréchet-type dendrimers with various groups at the end of the dendron as stabilizers for preparing metallic nanoparticles provides the advantage of minimal surface deactivation for catalytic applications. Pd and Pt nanoparticles that are stabilized by Fréchet-type dendrimers have been shown to efficiently catalyze Heck, Suzuki, and hydrogenation reactions [19, 31–33].

Au is one of two transition metals that is more electronegative than Pt and is useful as an alloying metal with

other metals, such as Pt or Pd, for various catalytic reactions [41, 42]. Pd/Au core/shell bimetallic nanoparticles have been observed as superior to monometallic Pd nanoparticles in the catalytic hydrogenation of allyl alcohol in water [43]. Pt/Au bimetallic nanoparticles with a 1:1 stoichiometry that were supported on silica were highly active for CO catalytic oxidation at room temperature [41].

In this paper, we report the preparation of Au/Pt bimetallic core/shell nanoparticles that are stabilized by Fréchet-type polyaryl ether trisacetic acid chloride dendrimer (G₃-NACl). The reason for using G₃-NACl as the stabilizer is that the dendrons can radically attach to the metal core, thus leaving a relative large fraction of surface of nanoparticles unpassivated and available for catalytic reactions [32]. The liquid phase hydrogenation of phenylaldehydes and nitrobenzenes was used to investigate the contribution of the gold component that is contained in the bimetallic nanoparticle to the catalytic activity. The results showed that Au/Pt core/shell bimetallic nanoparticles were more active than both monometallic platinum nanoparticles and the physical mixture of monometallic platinum and gold nanoparticles.

2 Experimental

2.1 Materials

HAuCl₄ and H₂PtCl₆ were obtained from the Shanghai Chemical Reagents Company. A polyaryl ether trisacetic acid ammonium chloride dendrimer was synthesized as described in Ref. [32].

2.2 Preparation of Au Monometallic Nanoparticles and Au/Pt Core/Shell Bimetallic Nanoparticles that are Stabilized by Polyaryl Ether Trisacetic Acid Ammonium Chloride Dendrons

Au nanoparticles that were stabilized by G₃-NACl were prepared using the alcohol reduction method under microwave irradiation [44]. In a typical experimental, 0.5 mL of 0.217 mmol/L G₃-NACl and 0.4 mL of 9.706 mmol/L HAuCl₄ were dissolved in 20 mL aqueous ethanol solution ($V_{water}/V_{ethanol} = 1$, the pH of the solution was adjusted to ∼9 with approximately 30 μL of dilute KOH solution) by ultrasonic treatment. Then, the mixture was irradiated with microwaves for about 20 s in a microwave oven (i.e., 2,450 MHz at the maximum power output of 700 W), which was retrofitted with the addition of a mechanical stirring apparatus. The color of the solution changed from light yellow to purplish after the irradiation. The core/shell bimetallic Au/Pt nanoparticles ($n_{Pt}/n_{Au} = 1$) were prepared by adding a mixture of 0.5 mL H₂PtCl₆ (7.723 mmol/L) and 0.25 mL G₃-NACl

(0.217 mmol/L) aqueous ethanol solution to the gold colloidal solution, followed by bubbling H₂ through the solution for 3 h. This resulted in a core/shell bimetallic colloidal solution. Bimetallic nanoparticles in various molar ratios of Pt and Au can be prepared by the same method by simply varying the amount of platinum that is added to the gold colloidal solution. The color of the resulting colloidal solution was dark red to dark brown, depending on the molar ratio of platinum and gold used for the preparation. The samples were labeled as Pt₁₀₀₋ₓAuₓ@G₃NACl, where x represents the number of gold atoms for every 100 platinum and gold atoms combined, and x can vary between 0 and 100.

2.3 Characterization

The UV-Vis absorption spectra of the samples were measured with a TU1810 SPC spectrophotometer. Transmission electron microscopy (TEM) studies were conducted with a TECNAI G20 electron microscope operating at an accelerating voltage of 200 kV. Samples for TEM analysis were prepared by dropping approximately 3 μL of diluted bimetallic colloidal solution onto carbon covered copper grids, and which was then allowed to air dry. The samples were kept into the desiccator prior to measurement. X-ray powder diffraction (XRD) was performed with a DMAX-3C Rigaku X-ray diffractometer with Cu Kα radiation, which was operated at an accelerating voltage of 30 kV and a current of 25 mA. The samples were prepared as a thin film on a glass plate by evaporating the solvent from the bimetallic colloids.

2.4 Hydrogenation Reactions

The hydrogenation reactions were carried out in a 50 mL three-necked round-bottom Schlenk flask that was equipped with a hydrogen adapter, a drop funnel, and a reflux condenser with a second adapter connected to a liquid paraffin bubbler. The system was purged with H₂ for 30 min before the reaction. The catalytic reactions were carried out by adding a proper amount of a substrate and the Au/Pt bimetallic colloidal solution through the drop funnel while stirring vigorously. The catalytic hydrogenation reactions were run under conditions of atmospheric pressure. The products of nitrobenzenes hydrogenation were identified with a GC-9800 gas chromatograph equipped with an FID detector and an SE-30 packed column, whereas the products of 3-phenoxybenzaldehyde hydrogenation were analyzed on the gas chromatograph with a capillary column. The catalytic hydrogenation process for 3-phenoxybenzaldehyde can also be conveniently monitored by the descent of the substrate absorption band that is centered at 306 nm on a UV-vis spectrophotometer.

3 Results and Discussions

3.1 Preparation and Characterization of Au Monometallic and Au/Pt Bimetallic Nanoparticles that are Stabilized by G3-NACl

The gold nanoparticles prepared by the alcohol reduction method under microwave irradiation demonstrated a Gaussian-like size distribution. The average diameter of the nanoparticles and dispersivity are 6.0 ± 2.3 nm (Fig. 1). The XRD pattern of the Au nanoparticles showed the characteristic diffraction peaks of the face-centered cubic phase of the metal. Diffraction peaks at $38.2°$ and $44.3°$ correspond to the diffractions of the (111) and (200) crystalline planes (Fig. 2 curve a). Peak broadening analysis on the (111) peak of the Au nanoparticles using Scherrer's equation indicated a grain size of approximately 6.5 nm, which is corresponds to the TEM result.

Au/Pt bimetallic nanoparticles with various Pt contents were prepared by dihydrogen reducing $HAuCl_4$ in the presence of Au nanoparticles. As dihydrogen gas was bubbled through the solution of H_2PtCl_6 and Au colloid, the color of the solution turned first from purplish to dark brawn and then to black. Figure 3 shows the UV-vis absorption spectra of the solution during the reduction process. The Au colloidal solution shows an absorption band at 540 nm, which corresponds to the typical surface plasmon resonance (SPR) of Au nanoparticles. Adding H_2PtCl_6 to the gold colloidal solution did not noticeably change the SPR peak of the solution. As Pt is deposited onto Au nanoparticles, the SPR peak at 540 nm gradually decreases, indicating the formation of Au/Pt nanoparticles that are stabilized by G3-NACl. Since the activation energy for heterogeneous nucleation is less than that for homogenous nucleation [10, 45] and gold nanoparticles can activate dihydrogen at the particle surface [46], we believe that Pt atoms mainly deposit on the surface of the gold
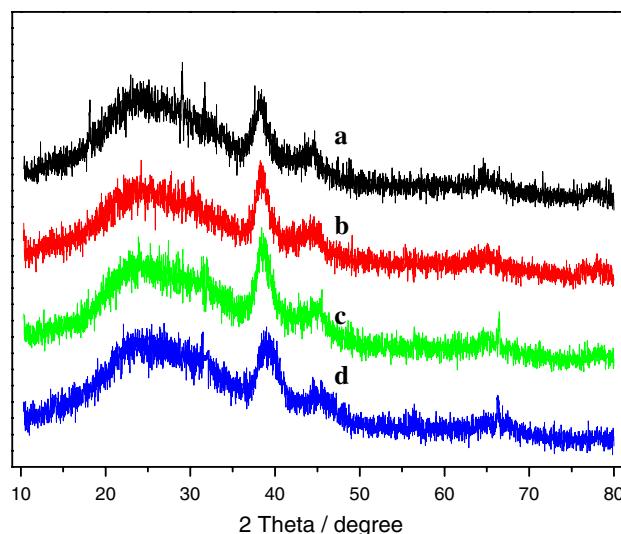

Fig. 2 XRD patterns of Au@G₃NACl (**a**), Pt₂₅Au₇₅@G₃NACl (**b**), Pt₅₀Au₅₀@G₃NACl (**c**), and Pt₇₅Au₂₅@G₃NACl (**d**)

nanoparticle, thereby forming core/shell bimetallic nanoparticles instead of discrete Pt nanoparticles.

Figure 4 presents the UV-vis spectra of Au/Pt bimetallic nanoparticles with various ratios of Au/Pt. As the Pt content of the bimetallic nanoparticles increased, the intensity of the SPR peak at 540 nm gradually decreased. The SPR peak disappeared completely when the molar ratio of Au/Pt reached one, and the spectra of the bimetallic Au/Pt colloidal solutions with high Au/Pt ratios are similar to that of the monometallic Pt colloidal solution.

A 6-nm gold nanoparticle that is treated as a central atom and surrounded by closed shells of identical atoms contains approximately 6,525 gold atoms [47]. One hundred percent Pt coverage on the gold nanoparticle is estimated to utilize 1,692 platinum atoms since Pt has an atomic radius (1.30 Å), which is very close to that of Au (1.34 Å). This means that the molar ratio of Pt/Au is about

Fig. 1 TEM image of Au@G₃NACl nanoparticles (**a**), and the corresponding size distribution histogram (**b**)
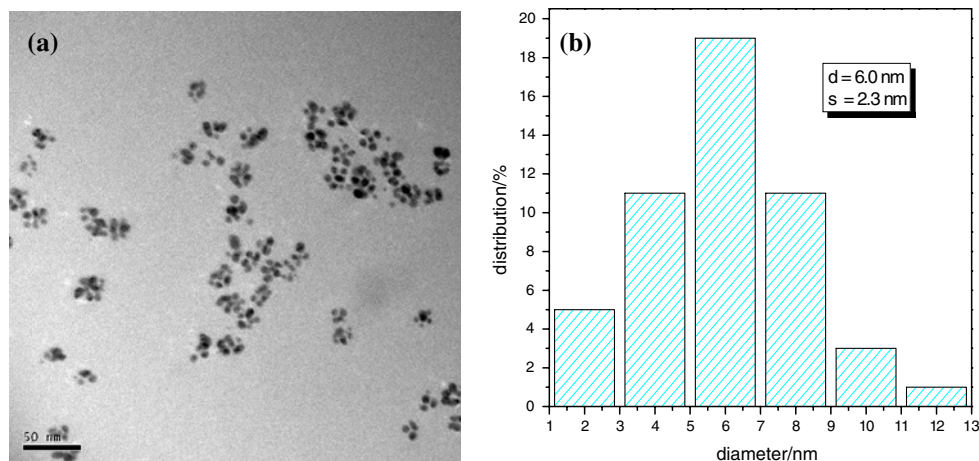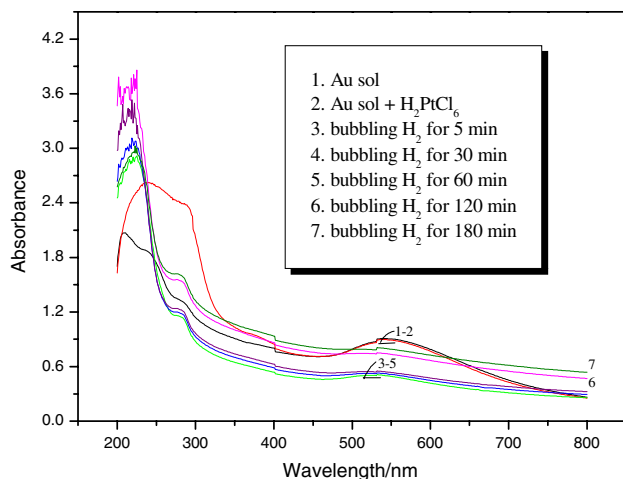
Fig. 3 UV-vis spectra of Au/Pt bimetallic nanoparticles during the reduction process
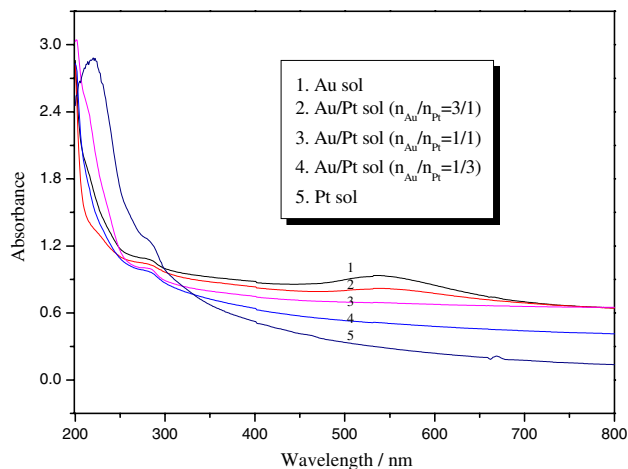

Fig. 4 UV-Vis spectra of Au, Pt monometallic, and Au/Pt bimetallic nanoparticles with various molar ratios of Au/Pt

26% for the case of one hundred percent Pt coverage on a 6-nm gold particle under ideal conditions. Crooks' group reported that in the UV-vis spectrum of Au/Ag bimetallic nanoparticles, a narrow SPR band corresponding to the Ag shell at 410 nm and a broader band at 510 nm arising from Au core were observed. Additionally, as the Ag content of the bimetallic nanoparticles increased to a definite value, only the Ag SPR band was observed in the absorption spectrum [37]. These observations are consistent with the results of the theoretic calculation that was performed by Liz-Marzan and Philipse [48]. This may be the same for Au/Pt bimetallic nanoparticles. With Pt relative lightly loaded on Au particles, the SPR band arising from Au core could still be observed since the surface of the gold core was only partially covered by platinum atoms; as the Pt content of the bimetallic nanoparticles increased to a definite value, the Au core would be completely covered by Pt

atoms, and the absorption spectrum of the bimetallic nanoparticles would become similar to that of Pt monometallic nanoparticles.

The XRD patterns for the Au/Pt bimetallic nanoparticles revealed that as the Pt/Au ratios increased from 1/3 to 1/1, the 2θ values of the XRD peaks shifted slightly toward higher values, indicating the formation of Pt on the Au seed (Fig. 2 curves b–c). However, when the molar ratio of Pt to Au reached 3, more broadened peaks were observed (Fig. 2 curve d), which may imply that some discrete Pt nanoparticles are formed in addition to Au/Pt bimetallic ones.

Transmission electron microscopy images of the bimetallic nanoparticles stabilized by G3-NACl and the corresponding size histograms are presented in Fig. 5. As shown by the TEM micrographs, the average size of the bimetallic nanoparticles was 9.0 ± 2.4 nm, 10.4 ± 2.8 nm, and 13.0 ± 3.2 nm for $Au_{75}Pt_{25}@G_3NACl$, $Au_{50}Pt_{50}@G_3NACl$, and $Au_{25}Pt_{75}@G_3NACl$, respectively. The results demonstrate that the average size of bimetallic nanoparticles increases as more Pt atoms deposit on the Au nanoparticles. However, the shape of $Au_{25}Pt_{75}@G_3NACl$ become irregular, and many fine particles (i.e., less than 2 nm) can be found on the image. The electron diffraction pattern taken from $Au_{75}Pt_{25}@G_3NACl$ nanoparticles (inset of Fig. 5a) shows the polycrystallinity of the bimetallic nanoparticles. The d spacings of 0.24, 0.21, 0.15, and 0.13 derived from the pattern confirm predominantly fcc structure.

3.2 Catalytic Hydrogenation of Au/Pt Bimetallic Nanoparticles

The catalytic hydrogenation of 3-phenoxybenzaldehyde to 3-phenoxyphenyl methanol and nitrobenzenes to anilines was investigated using bimetallic nanoparticles as catalysts. The catalytic hydrogenations were carried out under conditions of one atmosphere of hydrogen. The results from the catalytic hydrogenations using $Pt_{75}Au_{25}@G_3NACl$ as the catalyst are presented in Table 1. For comparison, the results of the catalytic hydrogenation using monometallic $Pt@G_3NACl$ nanoparticles as the catalyst under the same reaction conditions are also shown in the table. As shown in Table 1, the catalytic activity of the bimetallic $Pt_{75}Au_{25}@G_3NACl$ nanoparticles depends on the substrates. For the substrates of 4-nitrophenol and 2-methoxynitrobenzene, which are relatively easily hydrogenated to relative anilines, Au/Pt bimetallic nanoparticles do not exhibit notably higher catalytic activities than Pt monometallic nanoparticles. For catalytic hydrogenation of nitrotoluenes, the activity of the bimetallic nanoparticles of $Pt_{75}Au_{25}@G_3NACl$ is superior to that of the monometallic nanoparticles of $Pt@G_3NACl$. The conversions after 4 h of reaction time using
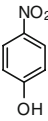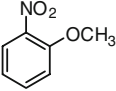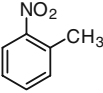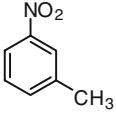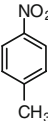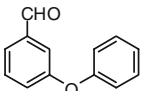
Fig. 5 HTEM images and the corresponding size distribution histograms of $Pt_{25}Au_{75}@G_3NACl$ (**a**), $Pt_{50}Au_{50}@G_3NACl$ (**b**), and $Pt_{75}Au_{25}@G_3NACl$ (**c**) bimetallic nanoparticles. Inset of (**a**) gives the corresponding electron diffraction pattern of $Pt_{25}Au_{75}@G_3NACl$
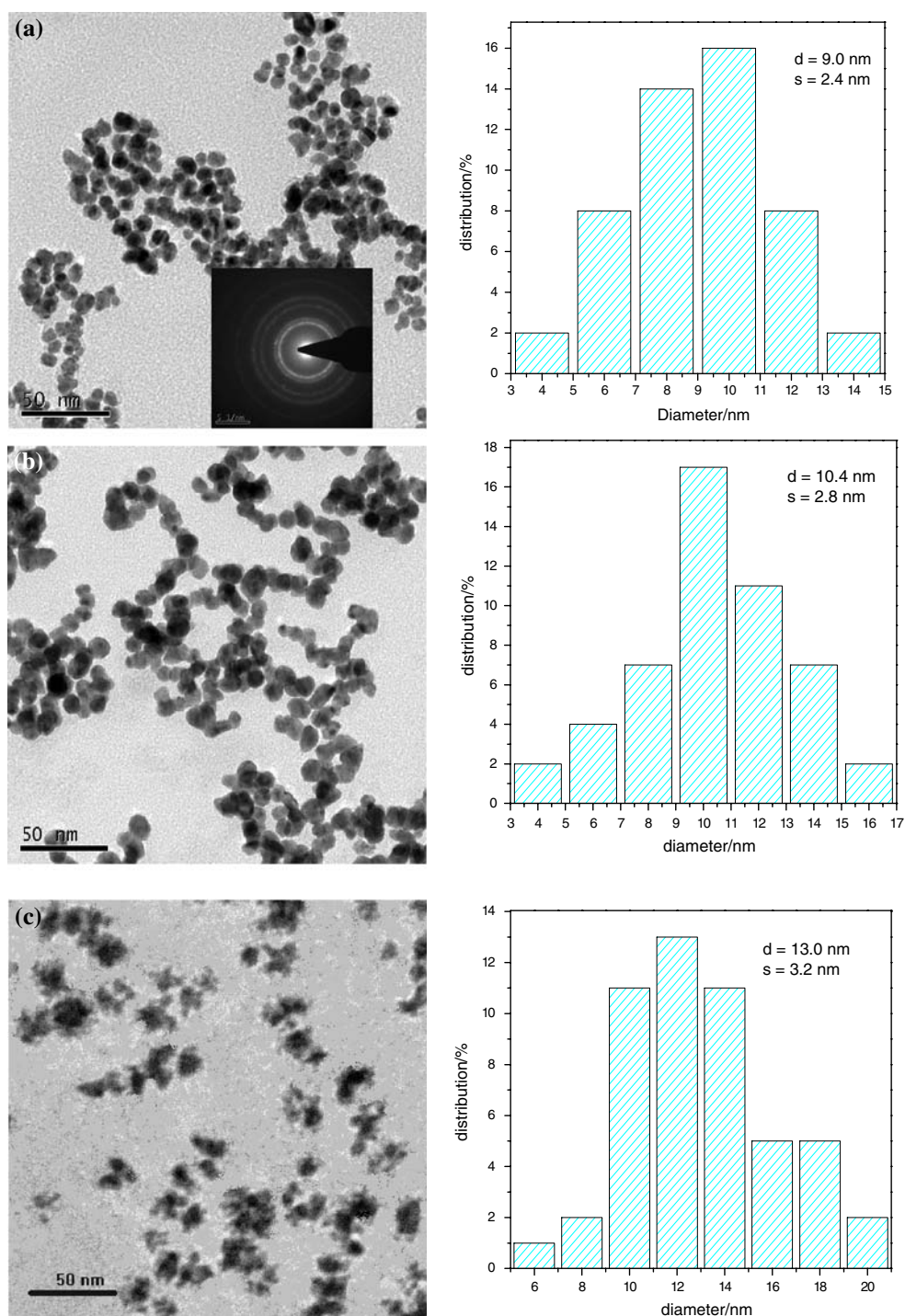
$Pt_{75}Au_{25}@G_3NACl$ as the catalyst are almost the same as those after 8 h of reaction time using $Pt@G_3NACl$ as the catalyst. The turnover frequencies (TOFs) of Au/Pt bimetallic nanoparticles are 112, 180, and 90 h^{-1} for o-, m-, p-nitrotoluene hydrogenation, respectively, which are approximately two times more than those of Pt monometallic nanoparticles. The temporal process of the hydrogenation of the nitrobenzenes catalyzed by $Pt_{75}Au_{25}@G_3NACl$ is shown in Fig. 6. For the 3-phenoxybenzaldehyde hydrogenation, the TOF of $Pt_{75}Au_{25}@G_3NACl$ bimetallic nanoparticles is greater than that of Pt nanoparticles under the same reaction conditions. The conversions of 3-phenoxy-benzaldehyde catalyzed by $Pt_{25}Au_{75}@G_3NACl$, $Pt_{50}Au_{50}@G_3NACl$, and $Pt_{75}Au_{25}@G_3NACl$ bimetallic nanoparticles versus reaction time are shown in Fig. 7. The results demonstrate that the activities of $Pt_{50}Au_{50}@G_3NACl$, and $Pt_{75}Au_{25}@G_3NACl$ nanoparticles are higher than that of $Pt_{25}Au_{75}@G_3NACl$

Table 1 Catalytic activity of $Pt_{75}Au_{25}@G_3NACl$ and $Pt@G_3NACl$ nanoparticles

Number	Substrate	Time (h)	Selectivity (%)	Conversion (%)	TOF ($n_{product}/n_{Pt} \cdot t$) $Pt_{75}Au_{25}@G_3NACl$	Time (h)	Selectivity (%)	Conversion (%)	TOF ($n_{product}/n_{Pt} \cdot t$) $Pt@G_3NACl$
1	(4-nitrophenol: NO_2, OH)	3.5	~100	~100	243	3.7	~100	~100	242
2	(NO_2, OCH_3)	4.0	~100	~100	232	4.0	~100	~100	224
3	(NO_2, CH_3)	4.0	~100	51	112	8.0	~100	60	64
4	(NO_2, CH_3)	4.0	~100	78	180	8.0	~100	77	95
5	(NO_2, CH_3)	4.0	~100	40	92	8.0	~100	49	49
6	(CHO, O-phenyl)	8.0	~100	75	91	8.0	~100	72	87

Reaction conditions-solvent: ethnol/water = 4(v/v); $n_{substrate}/n_{Pt}$ = 900; reaction temperature: 40 °C

nanoparticles, though the difference of the activities of $Pt_{50}Au_{50}@G_3NACl$ and $Pt_{75}Au_{25}@G_3NACl$ nanoparticles is not very obvious. These results may be interpreted as the surface of the gold core was only partially covered by platinum atoms in $Pt_{25}Au_{75}@G_3NACl$, while, the Au core was completely covered by Pt atoms in $Pt_{50}Au_{50}@G_3NACl$ and $Pt_{75}Au_{25}@G_3NACl$ nanoparticles.

3.3 Influence of Au Content in Au/Pt Bimetallic Nanoparticles on the Catalytic Hydrogenation

The catalytic hydrogenation of 3-phenoxybenzaldehyde to 3-phenoxyphenyl methanol was used to investigate the influence of Au content in Au/Pt bimetallic nanoparticles on the reactive activity. The activity of the catalytic hydrogenation varied significantly with the Au content in the Au/Pt bimetallic nanoparticles. Introducing Au into Pt nanoparticles markedly increased the reactive activity (Fig. 8). However, the activity decreased as the content of Au increased in the bimetallic nanoparticles (Fig. 8 curve a). The results from the catalytic activity of the physical mixtures of Pt and Au monometallic nanoparticles revealed that the activity of the catalytic hydrogenation basically linearly decreased with the increase in Au content (Fig. 8 curve b). Comparing the catalytic activities of the Au/Pt core/shell bimetallic nanoparticles with those of the mixture of Pt and Au monometallic nanoparticles, we find that the Au/Pt bimetallic nanoparticles are more active than the relative physical mixture of Pt and Au nanoparticles. The higher catalytic activity of the bimetallic
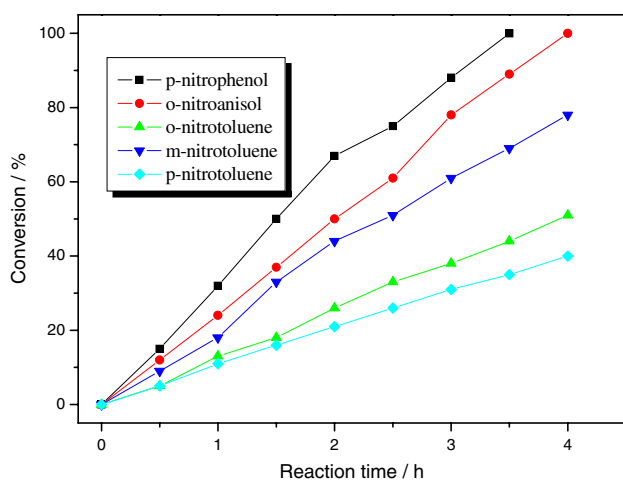
Fig. 6 The temporal process of the hydrogenation of the nitrobenzenes catalyzed by $Pt_{75}Au_{25}$@G_3NACl. Reaction conditions-solvent: ethnol/water = 4(v/v); $n_{substrate}/n_{catal}$ = 900; Reaction temperature: 40 °C

Fig. 7 Hydrogenation of 3-phenoxybenzaldehyde catalyzed by $Pt_{25}Au_{75}$@G_3NACl, $Pt_{50}Au_{50}$@G_3NACl, and $Pt_{75}Au_{25}$@G_3NACl. Reaction conditions- solvent: ethnol/water = 4(v/v); $n_{substrate}/n_{catal}$ = 900, Reaction temperature: 40 °C
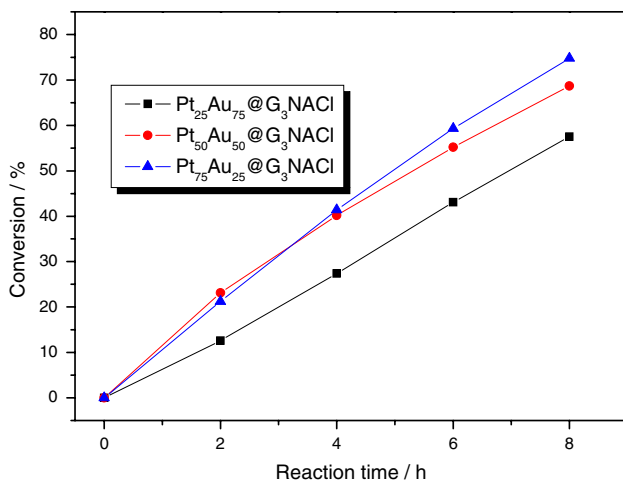
nanoparticles may be attributed to an ensemble effect between the Au and Pt atoms [8]. Since Pauling's electronegativity of gold (2.54) is larger than that of platinum (2.28), the interaction between these two different metals will allow the gold core to attract electrons from the platinum shell. The electron-deficient platinum shell of the bimetallic nanoparticles may favor the adsorption of the substrate with polar carboxyl groups. However, notably, Au/Pt alloy nanoparticles that are prepared by the co-reduction method are less active than Pt monometallic nanoparticles in catalytic hydrogenations [40]. The fact that Au/Pt alloy nanoparticles are less active may be attributed to a lesser availability of active sites left on the
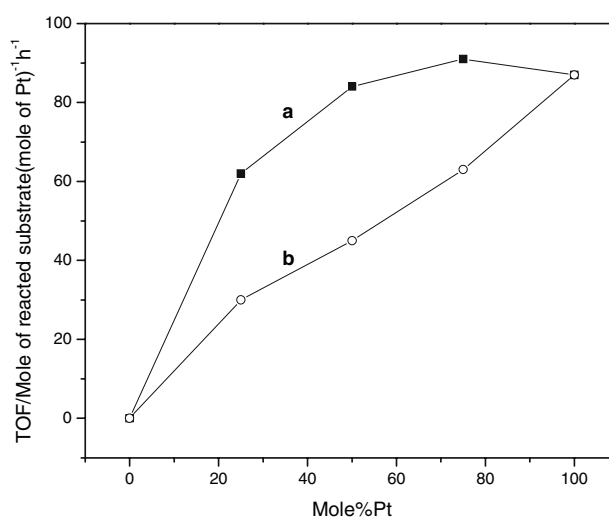

Fig. 8 Turnover frequencies (TOF) of 3-phenoxybenzaldehyde as a function of the molar ratio of platinum in Au/Pt bimetallic nanoparticles (**a**) and the physical mixtures of Pt and Au monometallic ones (**b**). Reaction conditions- $n_{substrate}/n_{catal}$ = 900, Reaction temperature: 40 °C, Reaction time: 8 h

surface of the alloy particles since gold atoms occupy some surface area of the nanoparticles.

4 Conclusions

Using a method of loading of platinum atoms on gold seeds that are the size of 6-nm, Au/Pt core/shell bimetallic nanoparticles stabilized by Fréchet-type polyaryl ether dendrimer with controlled Pt loading were successfully prepared. Au/Pt bimetallic nanoparticles showed higher catalytic activities for the hydrogenation of nitrotoluenes to anilines and 3-phenoxybenzaldehyde to 3-phenoxyphenyl methanol as compared to the monometallic platinum nanoparticles. Au/Pt core/shell nanoparticles also demonstrated higher catalytic activities than physical mixtures of monometallic Pt and Au nanoparticles. The Au core of the bimetallic nanoparticles promoted catalytic activity, which may be interpreted as an ensemble effect of the interaction between the gold core and the platinum shell, which results in an electron-deficient platinum shell on the nanoparticles.

References

1. Alexeev OS, Gates BC (2003) Ind Eng Chem Res 42:1571–1587
2. Sinfelt J (1987) Acc Chem Res 20:134
3. Raja R, Thomas JM (2002) J Mol Catal A: Chem 181:3

4. Johnson BFG, Raynor SA, Brown DB, Shephard DS, Mashmeyer T, Thomas JM, Hermans S, Raja R, Sankar G (2002) J Mol Catal A: Chem 182–183:89

5. Veisz B, Tóth L, Teschner D, Paál Z, Győrffy N, Wild U, Schlögl R (2005) J Mol Catal A: Chem 238:56

6. Guczi L, Beck A, Horváth A, Koppány Z, Stefler G, Frey K, Sajó I, Geszti O, Bazin D, Lynch J (2003) J Mol Catal A: Chem 204–205:545

7. Pronkin SN, Simonov PA, Zaikovskii VI, Savinova ER (2007) J Mol Catal A: Chem 265:141

8. Chung YM, Rhee HK (2003) J Mol Catal A: Chem 206:291–298

9. Villa A, Campione C, Prati L (2007) Catal Lett 115:133

10. Nutt MO, Heck KN, Alvarez P, Wong MS (2006) Appl Catal B Environ 69:115

11. Scott R, Datye A, Crooks R (2003) J Am Chem Soc 125:1757

12. Lu P, Teranishi T, Asakura K, Miyake M, Toshima N (1999) J Phys Chem B 103:9673

13. Rampino L, Nord F (1941) J Am Chem Soc 63:2745

14. Newkome G, Yao Z, Baker GR, Gupta VK (1985) J Org Chem 50:2003

15. Hawker CJ, Fréchet JMJ (1990) J Am Chem Soc 112:7638

16. Niu Y, Yeung L, Crooks R (2001) J Am Chem Soc 123:6840

17. Esumi K, Isono R, Yoshimura T (2004) Langmuir 20:237

18. Rahim E, Kamounah F, Frederiksen J, Christensen J (2001) Nano Lett 1:499

19. Gopidas K, Whitesell J, Fox M (2003) Nano Lett 3:1757

20. Gröhn F, Bauer BJ, Akpalu YA, Jackson CL, Amis EJ (2000) Macromolecules 33:6042

21. Ooe M, Murata M, Mizugaki T, Ebitani K, Kaneda K (2002) Nano Lett 2:999

22. Zhao M, Crooks R (1998) J Am Chem Soc 120:4877

23. Bhyrappa P, Young J, Moore J, Suslick K (1996) J Mol Catal A: Chem 113:109

24. Yang Z, Kang Q, Ma H, Li C, Lei Z (2004) J Mol Catal A: Chem 213:169

25. Koten G, Jastrzebski J (1999) J Mol Catal A: Chem 146:317

26. Touzani R, Alper H (2005) J Mol Catal A: Chem 227:197

27. Huang Y, Zhang H, Deng G, Tang W, Wang X, He Y, Fan Q (2005) J Mol Catal A: Chem 227:91

28. Mizugaki T, Ooe M, Ebitani K, Kaneda K (1999) J Mol Catal A: Chem 145:329

29. Smith G, Mapolie S (2004) J Mol Catal A: Chem 213:187

30. Yi B, Fan Q, Deng G, Li Y, Qiu L, Chan A (2004) Org Lett 6:1361

31. Du Y, Zhang W, Wang X, Yang P (2006) Catal Lett 107:177

32. Yang P, Zhang W, Du Y, Wang X (2006) J Mol Catal A: Chem 260:4

33. Zhang W, Du Y, Hua N, Wang X, Yang P (2006) Chinese J Inorg Chem 22:263

34. Li X, Du Y, Tao J, Wang X, Yang P (2007) Catal Lett 118:151

35. Ropartz L, Foster DF, Morris RE, Slawin AMZ, Cole-Hamilton DJ (2002) J Chem Soc, Dalton Trans, 1997

36. Tomalia DA, Naylor AM, Goddard WAIII (1990) Angew Chem Int Ed Engl 29:138

37. Wilson O, Scott R, Garcia-Martinez J, Crooks R (2005) J Am Chem Soc 127:1015–1024

38. Scott R, Datye A, Crooks R (2003) J Am Chem Soc 125:3708–3709

39. Chung Y, Rhee H (2003) Catal Lett 85:159–164

40. Li X, Li B, Cheng M, Du Y, Wang X, Yang P (2008) J Mol Catal A: Chem 284:1–7

41. Lang H, Maldonado S, Stevenson K, Chandler B (2004) J Am Chem Soc 126:12949–12956

42. Villa A, Campione C, Prati L (2007) Catal Lett 115:133–136

43. Scott R, Wilson O, Oh S-K, Kenik E, Crooks R (2004) J Am Chem Soc 126:15583–15591

44. Shen M, Du YK, Hua NP, Jiang L, Yang P (2006) Powder Technol 162:64–72

45. Kashchiev D, Rosmalen G (2003) Cryst Res Technol 38:555–574

46. Gluhoi AC, Vreeburg HS, Bakker JW, Nieuwenhuys BE (2005) Appl Catal A Gen 291:145–150

47. Schmid G (1992) Chem Rev 92:1709–1727

48. Liz-Marzan L, Philipse A (1995) J Phys Chem 99:15120–15128